International Journal of Concrete Structures and Materials

RESEARCH

Open Access

Investigation of Conditions for Using Mass-Produced Waste Glass as Sustainable Fine Aggregate for Mortar

Minjae Son[1], Gyuyong Kim[2*], Sangkyu Lee[1], Hongseop Kim[1], Hamin Eu[2], Yaechan Lee[2], Sasui Sasui[2] and Jeongsoo Nam[2]

Abstract

To address the environmental issues arising from the growing scarcity of natural fine aggregates (NFA) and landfilling of waste glass, research is being conducted globally to utilize waste glass as a sustainable fine aggregate. However, contradictory results have been obtained regarding the effect of the type of waste glass and the physical properties of waste glass fine aggregate (GFA) on concrete, making it challenging to promote the use of GFA in concrete. Therefore, to promote the use of GFA in concrete, it is necessary to examine it under field conditions, such as mass-production processes or real-scale concrete applications. This study introduced a mass-production process for GFA, and the effect of mass-produced GFA on mortar was evaluated. The fine aggregate properties (particle aspect ratio, crushing rate, and solubility) of the GFA and the effects of color, content, and particle size on the mortar properties (compressive strength, flexural strength, and ASR expansion behavior) were analyzed, along with the results reported in previous studies. Consequently, the high aspect ratio and microcracks in the particles of mass-produced GFA led to an increase in the strength reduction and ASR expansion of the mortar. These effects appear to be particularly severe for transparent GFA. Overall, this study proposed the content of GFA within 20% or the replacement of fine particles (< 500 μm) in NFA as a condition for sustainable fine aggregate.

Keywords Sustainable fine aggregate, Waste glass fine aggregate, Mass-production process, Aspect ratio, Microcracks, ASR expansion

1 Introduction

Concrete is an important construction material in social infrastructure (Son et al., 2021). The scarcity of natural fine aggregates (NFA) is increasing owing to the growing demand for concrete worldwide (Tamanna et al., 2020). Therefore, sustainability of construction materials is an important issue (Bilodeau & Malhotra, 2000). The landfilling of waste glass is an environmental issue that cannot be ignored (Hamada et al., 2022). Only 21% of the 130 million tons of glass produced worldwide is recycled (Soroushian & Sufyan, 2021). In 2018, 20.65 million tonnes of waste glass were produced in the European Union, and 4.9 million tonnes of waste glass were landfilled in the United States. Excluding unidentified amounts, 13,000 tons of waste glass will not be recycled in South Korea in 2022 (Lee et al., 2023). Although recycling capabilities vary depending on the country, an efficient method is required to resolve landfill waste glass.

Recently, many studies have proposed various applications for recycling waste glass as construction materials (Eu et al. 2024; Sasui et al., 2021, 2022). In

Journal information: ISSN 1976-0485 / eISSN 2234-1315

*Correspondence:
Gyuyong Kim
gyuyongkim@cnu.ac.kr
[1] Korea Institute of Civil Engineering and Building Technology, 283, Goyang-Daero, Ilsanseo-Gu, Goyang-Si 10223, Republic of Korea
[2] Department of Architectural Engineering, Chungnam National University, Daejeon 34134, Republic of Korea

particular, recycling waste glass as fine aggregate (FA) for concrete is attracting attention because its chemical composition is similar to that of NFA (Guo et al., 2020; Tamanna et al., 2020). The advantages of recycling waste glass as FA are as follows: (1) there is no need to melt the waste glass, which simplifies processing; (2) a significant amount of waste glass can be consumed by using it in concrete; (3) toxic substances (such as lead oxide and heavy metal ions) that may be contained in waste glass can become trapped in hardened concrete; and (4) the impermeable surface properties of waste glass can delay the penetration of concrete deterioration factors, such as chloride ions and sulfates. Therefore, using waste glass in concrete to replace NFA is an attractive approach to address the sustainability of construction materials and waste glass landfills. Various studies have been conducted on the use of waste glass as FA in concrete (Harrison et al., 2020; Khan et al., 2020). The effects of waste glass fine aggregate (GFA) on the mechanical properties and alkali-silica reaction (ASR) have been intensively investigated.

Previous studies have reported that GFA has contradictory effects on the mechanical properties (i.e., compressive and flexural strengths) of concrete. Some researchers have reported that GFA improves the mechanical properties of concrete (Corinaldesi et al., 2005; Penacho et al., 2014; Shayan & Xu, 2004). This appeared to be because the adhesion strength between the matrix and particles increased owing to the pozzolanic reaction of the GFA (Bisht & Ramana, 2018; Shayan & Xu, 2004). On the other hand, some researchers have reported that GFA has a negative effect on the mechanical properties of concrete (Bhandari & Tajne, 2013; Limbachiya, 2009; Park & Lee, 2004). This result was attributed to the smooth surface and sharp angular shape of the GFA (Tan & Du, 2013). The reason for these contradictory effects is that the GFA used in previous studies had different characteristics, such as type (color), content, and particle size.

Because the amorphous silica in GFA is well-known and can potentially deteriorate the ASR of concrete, numerous studies have been conducted under the conditions of GFA, such as the effect of type (color), content, and particle size. However, the effect of GFA on the ASR of concrete has yielded contradictory results. In some studies, the ASR expansion of GFA according to color was in the order transparent > brown > green (Değirmenci et al., 2011; Jin et al., 2000; Topçu et al., 2008; Yuksel et al., 2013; Zhu et al., 2009). However, other studies have reported contradictory results. Compared with the other colors, clear glass showed the least ASR expansion (Dhir et al., 2009). A lower ASR expansion was observed for brown glass than green glass (Du & Tan, 2013, 2014a, 2014b). There are also debates about the effect of GFA content on the ASR expansion of concrete. Some researchers have reported that increasing the GFA content results in high ASR expansion (Kou & Poon, 2009; Ling & Poon, 2011; Serpa et al., 2013). In contrast, some researchers have reported that increasing the GFA content does not contribute to ASR expansion (Dhir et al., 2009; Du & Tan, 2014a, 2014b; Ismail & Al-Hashmi, 2009; Zhu et al., 2009). The effect of GFA particle size on the ASR expansion of concrete was found to be similar (Idir et al., 2010; Rajabipour et al., 2010; Xie et al., 2003). The results showed that the ASR expansion of the concrete decreased as the particle size decreased. On the other hand, studies still reported different "threshold sizes," which did not significantly affect ASR expansion. Threshold sizes have been variously reported as 0.3 mm (Jin et al., 2000; Xie et al., 2003), 0.6 mm (Rajabipour et al., 2010), 1 mm (Idir et al., 2010) and 1.18 mm (Du & Tan, 2013). Moreover, the critical particle size for the pozzolanic reaction was observed to be different: 0.15–0.30 mm (Yamada & Ishiyama, 2005) or 0.6–1.18 mm (Idir et al., 2010; Jin et al., 2000; Xie et al., 2003).

The causes of these research gaps have been suggested as follows: the types of waste glass used in the production of GFA (e.g., chemical composition and glass manufacturing process) (Dhir et al., 2009; Park & Lee, 2004) and the crushing process for the preparation of GFA (Du & Tan, 2013, 2014a, 2014b; Wang et al., 2022a, 2022b). Glass exhibits different strengths and solubilities depending on its purpose, owing to the different chemical compositions and production conditions. For instance, the leaching rate of glass is significantly influenced by its thermal history, and annealed glass has a lower leaching rate (Charles, 1958). Moreover, the physical properties of GFA, such as the particle size distribution, shape, and roughness, may vary depending on the crushing method (Wang et al., 2022a, 2022b). Research gaps regarding the effectiveness of GFA create difficulties in promoting their use in concrete (Guo et al., 2020). Therefore, some researchers have reported that to utilize GFA as a sustainable construction material, it is necessary to examine it under field conditions rather than laboratory conditions (Dadouch et al., 2024; Wang et al., 2022a, 2022b). However, few studies have investigated the processes that enable the mass production of GFA as a construction material and the effects of mass-produced GFA on concrete. For GFA to be utilized as a construction material, it is necessary to understand the effect of mass-produced GFA on cement-based composite materials.

Therefore, in this study, a mass-production process for GFA was introduced, and the FA properties of the mass-produced GFA were investigated. In addition, the effects of color, content, and particle size on the compressive

strength, flexural strength, and ASR expansion of the mortar were evaluated. The effects of the mass-production process of GFA are discussed by comparing the experimental results with those presented in previous studies.

2 Experimental Program

2.1 Waste Glass Fine Aggregate And Material

In Korea, waste glass is collected by local governments and private collection companies and transferred to intermediate processing companies (Lee et al., 2023). Waste glass collected by intermediate processing companies can be considered to satisfy the purpose of this study (GFA under field conditions) because it is not limited to a specific type and contains a mixture of various types. Therefore, this study used waste glass from an intermediate processing company to manufacture FA, as shown in Fig. 1. Waste glass is sprayed with water to remove foreign substances (such as dust) and contaminants before production.

In this study, a production process (performed by Indong GRC Company in Gunsan-si, Korea, an intermediate processing company) was used to obtain mass-produced GFA, as shown in Fig. 2. The detailed production process is as follows: (1) Picking up foreign substances by hand from waste glass, which is provided in fixed quantities from automatic feeders; (2) Separate metal products (such as bottle caps) with a magnetic separator; (3) Sieving particles using a trommel screen (≤ 5 mm); (4) Particles (>5 mm) are crushed through a hammer crusher (a 10 mm screen is installed), and glass powder generated during the crushing process is collected through a separate dust collector; (5) The particles crushed by the hammer crusher were re-sieved using a trommel screen (≤ 5 mm); (6) For non-sieved particles (>5 mm), repeat the crushing process with a hammer crusher; (7) Sieved particles (≤ 5 mm) undergo additional processes such as magnetic separation, eddy current separation, and air separation; (8) The separated particles are secondary crushed with a roll crusher (The gap size of roll is 2 mm) and then mixed with glass powder to produce GFA.

This process is similar to the recycled waste glass production process used by intermediate processing companies in Korea (Lee et al., 2023). However, in this study, additional processes were added to produce GFA. The hammer crusher produced waste glass particles within 5 mm, which was insufficient to meet the FA particle size distribution standards. Therefore, the waste glass particles were subjected to secondary crushing using a roll crusher to satisfy the particle size distribution standards. During the separation, approximately 5 wt. % of foreign substances were removed from the total waste glass, and it was confirmed that 50–80 tons/day of GFA can be produced through the production process.

The colors of waste glass collected by intermediate processing companies are mainly transparent (clear), green, and brown; however, there are also some special colors, such as blue and purple. Special glass colors were not considered; this study used three colors (transparent, green, and brown) as the GFA. To avoid limiting the use of certain types of glass, GFA was obtained by appropriately mixing 10 bulks (1 ton) of each color. Mixed GFA was manufactured by mixing GFA of each color at the same content, as shown in Fig. 3. Although in this study, GFA was manufactured from waste glass of the same color to investigate the effect of glass color, the

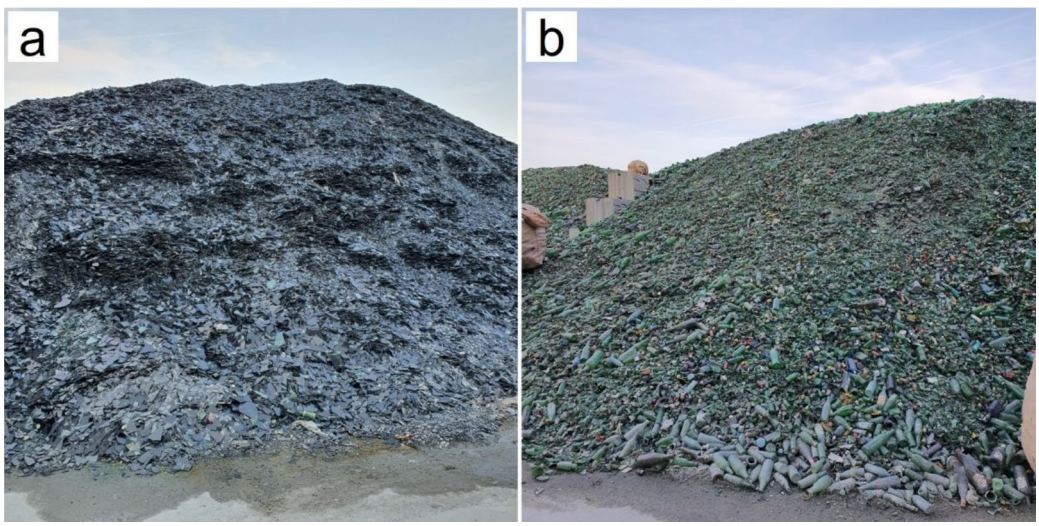

Fig. 1 Image of waste glass for fine aggregate (**a** Plate glass, **b** Bottle glass)

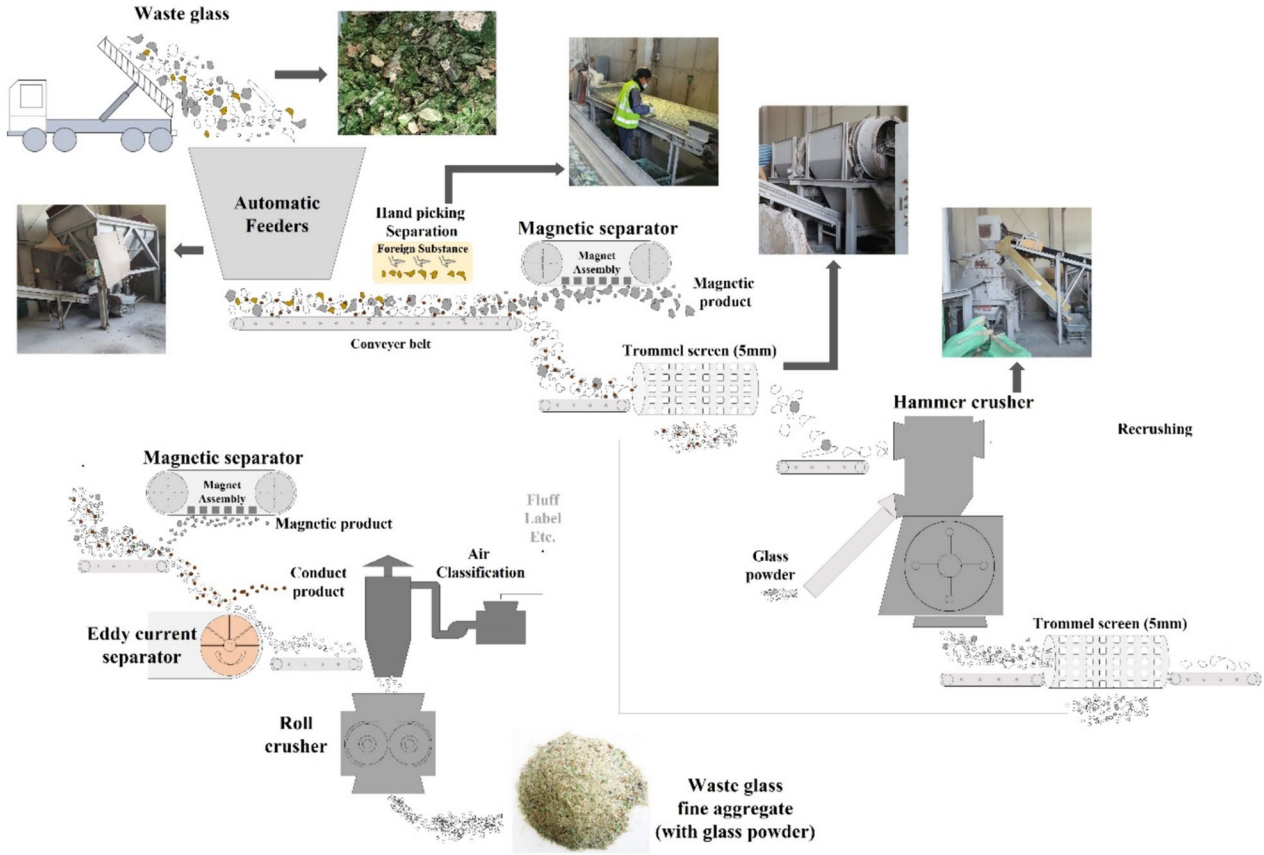

Fig. 2 Manufacturing process of waste glass fine aggregate

production process (Fig. 2) can also be applied to waste glass that cannot be recycled because of its mixed colors.

In this study, the prepared GFA were not washed separately. GFA satisfies the standard for the impurity content of recycled aggregates (KS F 2576) by removing foreign substances through various separation processes (Fig. 2) (Lee et al., 2023). The NFA used river sand, and the particle size distribution of the Mixed GFA is shown in Fig. 4. The mixed GFA satisfied FA particle size distribution standards (KS F 2527 2007). Therefore, the possibility of the continuous production of GFA of similar quality was confirmed, which can be considered to meet the purpose of this study. The other colors of the GFA showed a particle size distribution similar to that of the Mixed GFA. However, to eliminate the effect of particle size, the particle size distribution of the GFA of different colors was set to be the same based on the Mixed GFA.

Table 1 shows the chemical composition of the FA. GFA can be considered a soda-lime type because it consists of approximately 65% SiO_2, 13% CaO, and 11% Na_2O (Shi & Zheng, 2007). The waste glass used in this study was household waste, primarily windows, bottles, jars, and containers, which are reported to be a type of soda lime (Siddique, 2008). While no Cr_2O_3 was observed in the transparent GFA, the green and brown GFA contained Cr_2O_3 contents of 0.21% and 0.04%, respectively, similar to those reported by other researchers (Jin et al., 2000; Park & Lee, 2004). Notably, transparent GFA showed half the level of Fe_2O_3 compared to GFA of other colors, which appears to be intended to improve the transparency of the glass (Kaewkhao et al., 2011). The density of NFA and GFA were similar at 2.54 and 2.45 g/cm^3, respectively, but the water absorption rates were 1.6 and 0.4%, respectively. GFA has a lower water absorption rate than NFA because of its impermeable surface (Taha & Nounu, 2008, 2009). Ordinary Portland cement with a density of 3.15 g/cm^3, a specific surface area of 3,200 cm^2/g, and an equivalent alkali content of 0.6% was used.

2.2 Experimental Plan

In this study, the properties of mass-produced GFA were investigated. As FA properties, aspect ratios according to the particle size, solubility, and aggregate crushing rate, were investigated. Additionally, the GFA conditions were classified to evaluate the effects of GFA on the mortar. Compressive, flexural, and accelerated mortar bar tests

Fig. 3 Shape of waste glass fine aggregate (**a** Transparent, **b** Green, **c** Brown, **d** Mixed)

(AMBT) of the mortars were performed according to the color, content, and particle size of the GFA. The particle size classes and mass of GFA used in the compressive and flexural tests and the particle size effect (AMBT), are listed in Table 2. Five classes were investigated to evaluate the effect of particle size, which are 4.75–2.36 mm (S1), 2.36–1.18 mm (S2), 1.18–0.6 mm (S3), 600–300 μm (S4), and 300–150 μm (S5). For the mass settings of the classes, the NFA mass was used for the compressive and flexural tests, and the mass required by ASTM C 1260 was used for the AMBT. The particle size of 150–0 μm (S6) was not considered, as it has a low mass (2%) and is well known to cause pozzolanic reactions (Shao et al., 2000).

The mix proportion of the mortar for the compressive and flexural tests was selected according to ASTM C 109 with water:cement:FA ratio of 0.485:1:2.75. Mortar specimens were prepared in three series (color, content, and particle size), and the detailed mix proportions for the compressive and flexural tests are listed in Table 3. The sustainable conditions of GFA for cement-based composites were investigated. The contents of 10, 20, 30, 40, and 50% of GFA were replaced by NFA, referring

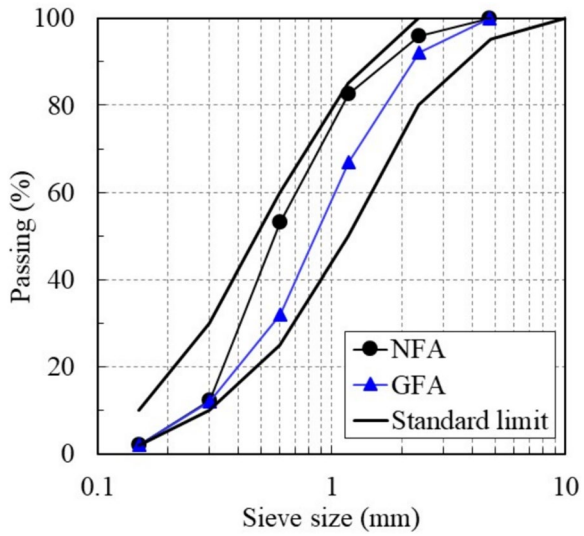

Fig. 4 Particle size distribution of fine aggregate

to other studies (Corinaldesi et al., 2005; Kou & Poon, 2009; Limbachiya, 2009; Penacho et al., 2014; Serpa et al., 2013), where the mass of each particle size of NFA was 100% replaced by GFA, denoted as S1, S2, S3, S4, and S5, respectively.

The mortar mix proportion for the AMBT was selected according to ASTM C 1260, with water:cement:FA ratio of 0.47:1:2.25. Similar to the compressive and flexural tests, three series of mortar specimens for the AMBT were prepared, as shown in Table 4.

2.3 Test Method

2.3.1 Image Analysis for Aspect Ratio

The FA particle shape has various effects on cement-based composites (Guinea et al., 2002; Jiang et al., 2021). Therefore, in this study, the aspect ratio was analyzed according to the particle size of the FA. The aspect ratio was measured using ImageJ, which allows for measuring and analyzing parameters such as length and area in the images. Fig. 5 shows an overview of the FA measurements using ImageJ. Image preprocessing is required for measurement; the background and shadows are removed, clarity is improved, and binary mode transformation is performed for accurate segmentation of particle boundaries. After image preprocessing, the parameters were automatically measured using the program, and the aspect ratio of the particles was calculated using the following equation (Matsumoto et al., 2015):

Table 1 Chemical composition of fine aggregates

Chemical composition (%)	Natural fine aggregate (NFA)	Waste glass fine aggregate (GFA)			
		Transparent (Tr)	Green (Gr)	Brown (Br)	Mixed
SiO_2	81.21	64.35	65.93	66.98	65.91
Al_2O_3	9.12	3.95	4.09	4.25	3.93
Fe_2O_3	2.15	0.39	0.65	0.63	0.43
CaO	2.41	13.60	12.95	11.39	12.95
MgO	0.83	0.73	1.43	1.39	1.42
Na_2O	1.91	9.93	11.67	11.73	10.23
K_2O	1.62	0.89	1.16	1.23	0.98
Cr_2O_3	–	–	0.21	0.04	0.12
NiO	–	–	0.01	0.01	–
CuO	–	–	0.01	0.01	–

Table 2 Particle size classes of fine aggregate and mass of each particle

Particle size classes		S1	S2	S3	S4	S5	S6
Sieve size		#4–8	#8–16	#16–30	#30–50	#50–100	<#100
Passing		4.75 mm	2.36 mm	1.18 mm	600 µm	300 µm	150 µm
Retained on		2.36 mm	1.18 mm	600 µm	300 µm	150 µm	0 µm
Mass (%)	Compressive and flexural test	4	13	30	41	10	2
	AMBT	10	25	25	25	15	–

Table 3 Mix proportions of mortar for the compressive and flexural test

Usage condition	ID	Water (g)	Cement (g)	Fine aggregate (g)					Notes
				NFA	GFA				
					Tr	Gr	Br	Mixed	
Color	Ref	242	500	1375					
	Tr				1375				
	Gr					1375			
	Br						1375		
	Mixed							1375	Same as 100%
Content	10%			1237.5				137.5	
	20%			1100				275	
	30%			787.5				412.5	
	40%			962.5				550	
	50%			687.5				687.5	
Particle size	S1			1320				55	Used GFA: #4–8
	S2			1196.25				178.75	Used GFA: #8–16
	S3			787.5				412.5	Used GFA: #16–30
	S4			811.25				563.75	Used GFA: #30–50
	S5			1237.5				137.5	Used GFA: #50–100

Table 4 Mix proportions of mortar for the AMBT

Usage condition	ID	Water (g)	Cement (g)	Fine aggregate (g)					Notes
				NFA	GFA				
					Tr	Gr	Br	Mixed	
Color	Ref	235	500	1125					
	Tr				1125				
	Gr					1125			
	Br						1125		
	Mixed							1125	Same as 100%
Content	10%			1012.5				112.5	
	20%			900				225	
	30%			787.5				337.5	
	40%			675				450	
	50%			562.5				562.5	
Particle size	S1			1012.5				112.5	Used GFA: #4–8
	S2			843.75				281.25	Used GFA: #8–16
	S3			843.75				281.25	Used GFA: #16–30
	S4			843.75				281.25	Used GFA: #30–50
	S5			956.25				168.75	Used GFA: #50–100

$$\text{Aspect ratio} = \frac{1}{4} \times \frac{\pi \times [Major \cdot axis]^2}{[Area]} \quad (1)$$

The aspect ratios of the NFA, transparent GFA (GFA_Tr), green GFA (GFA_Gr), and brown GFA (GFA_Br) were analyzed with 100 particles of each particle size (S1, S2, S3, S4, and S5).

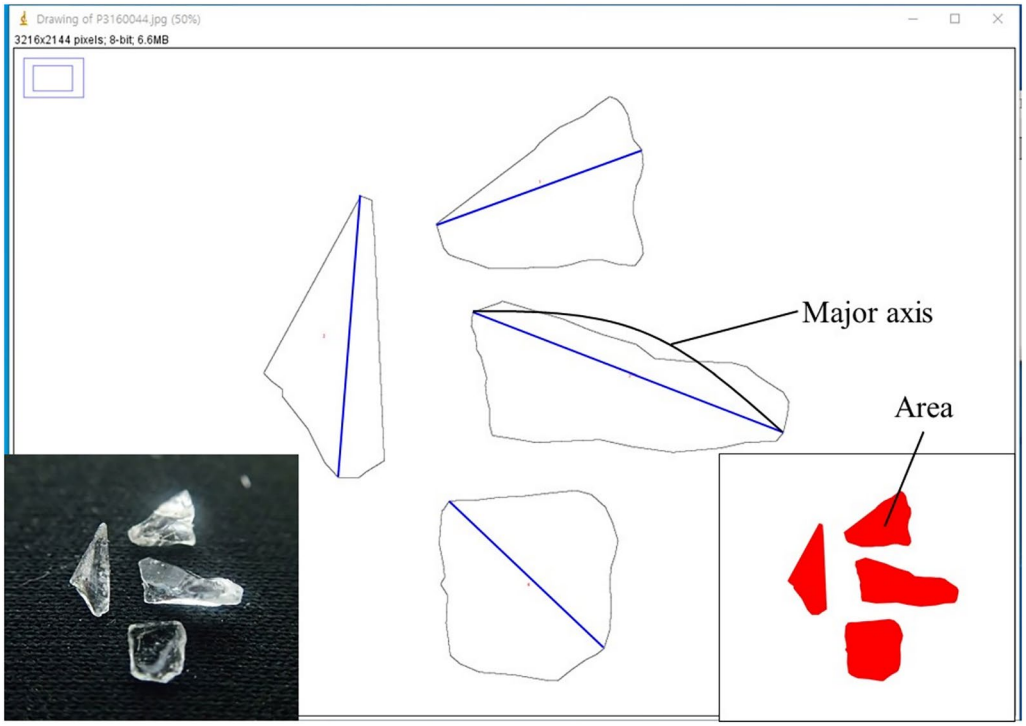

Fig. 5 Overview of length and area measurement of fine aggregate using Image J program

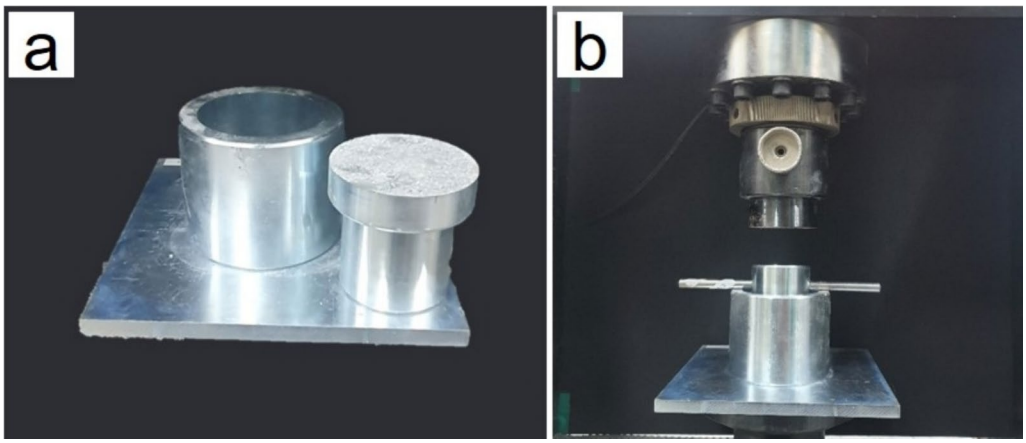

Fig. 6 Crushing rate test (**a** Cylinder and plunger, **b** Overview of the test)

2.3.2 Crushing Rate

The FA crushing rate was determined in accordance with KS F 2541 (2022). Although KS F 2541 is a test method for measuring the crushing rate of coarse aggregates, it was used in this study because it presents a test method for aggregate particles of 4.75–3.35 mm. Fig. 6 shows the equipment and outline for the crushing rate test. A cylinder (inner diameter 75 mm) was filled with 200 g of FA of 4.75–3.35 mm, and a load of 10 kN/min was applied using a plunger for 10 min. After applying the load, the mass of the particles sieved through a 0.85 mm sieve was measured. The crushing rate of the FA was calculated using the following equation:

$$G_f = \frac{A}{B} \times 100 \tag{2}$$

where G_f is the fine aggregate crushing rate (%), A is the mass of aggregate passed through a sieve of 0.85 mm (g), B is the mass of the sample at surface dry saturation (g)

The crushing rate test was performed five times for each FA (NFA, GFA_Tr, GFA_Gr, and GFA_Br).

2.3.3 Solubility

Waste glass has been reported to have different alkali reactivities depending on its color (Değirmenci et al., 2011; Topçu et al., 2008; Yuksel et al., 2013). Therefore, the solubility of GFA in an alkaline solution was evaluated using a test method (Saccani & Bignozzi, 2010). 1 kg of GFA (particle size of 4.75–3.35 mm) for each color was stored in 1 L of alkaline solution (1 N NaOH) at 80 °C in static mode. The weight loss (%) of GFA was recorded at 3, 7, 10, and 14 days after immersion. The solubility tests were performed five times for each GFA (GFA_Tr, GFA_Gr, and GFA_Br).

2.3.4 Compressive and Flexural Test

Compressive and flexural tests were performed to evaluate the effect of the GFA on the mechanical properties of the mortar. Compressive and flexural tests were conducted according to ASTM C 109 (2008) and 348 (2008), respectively. Five cubic ($50\times50\times50$ mm^3) and five mortar bars ($40\times40\times160$ mm^3) were evaluated for the compressive and flexural tests, respectively.

2.3.5 Accelerated Mortar Bar Test (AMBT)

A method for measuring the ASR expansion via AMBT is described in ASTM C 1260 (2014). Five mortar bars ($25\times25\times285$ mm^3) were demolded 1 d after casting and stored in water at 80 °C for 1 d. After measuring the initial length, the mortar bar was immersed in 1N NaOH solution at 80 °C, and the expanded length was measured every day thereafter. Three mortar bars were evaluated for the AMBT. In ASTM C 1260, if the expansion is less than 0.1% at 14 days, it is defined as innocuous. However, some studies have reported that mortars using GFA may exhibit rapid expansion after 14 days (Du & Tan, 2013, 2014a, 2014b). Therefore, the AMBT was performed for up to 28 days.

3 Results and Discussion

3.1 Fine Aggregate (FA) Properties

Fig. 7 shows the shapes of the GFA obtained using a scanning electron microscope. Smooth surfaces and angled shapes were observed in the GFA, regardless of color. However, a rough surface (Fig. 7c) was observed on some particles because the GFA was not washed separately in this study. Compared with the other colors, GFA_Tr showed numerous micro-damages (such as cracks) on the surface, as reported in some studies (Rajabipour et al., 2010; Tan & Du, 2013). The low Fe_2O_3 content in glass causes a decrease in the strength owing to the weak glass network (Li et al., 2022). Therefore, it appears that numerous micro-damages occurred in GFA_Tr. However, microdamage was not observed in GFA_Gr and Br, as shown in the SEM micrographs.

The aspect ratio according to the particle size of FA is shown in Fig. 8a. S3-5 tends to have a higher aspect ratio than S1-2, regardless of the FA type. This indicated that smaller particles were more likely to have sharp and angular shapes. Regardless of the particle size, all GFAs exhibited higher aspect ratios than

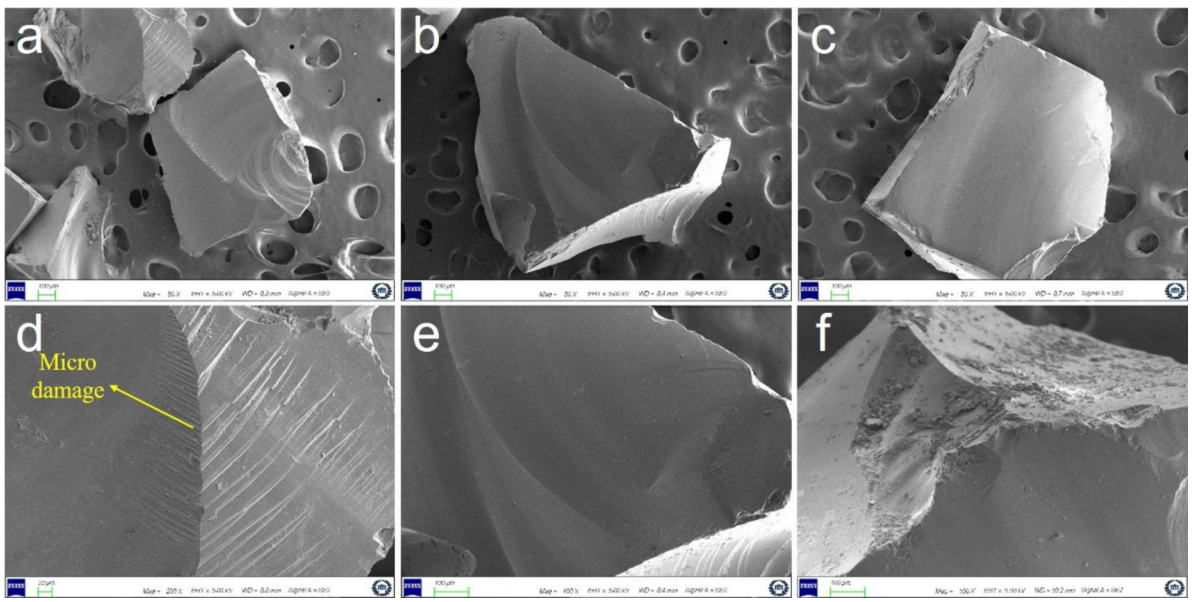

Fig. 7 SEM micrographs of GFA (**a, d** Transparent, **b, e** Green, **c, f** Brown)

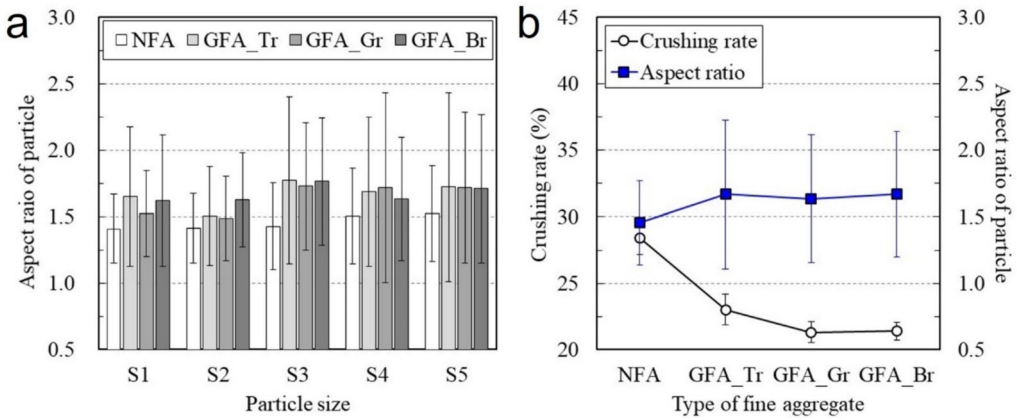

Fig. 8 Physical properties of FA (**a** Aspect ratio of the particle, **b** Aspect ratio and crushing rate)

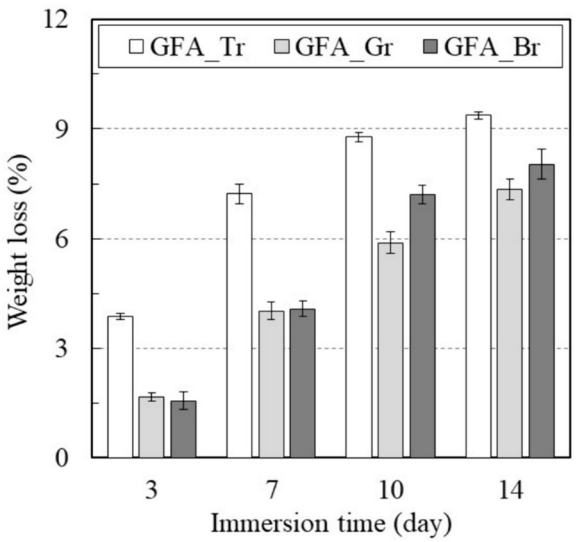

Fig. 9 Solubility of GFA in 1N NaOH solution

the NFA. In particular, the largest aspect ratio difference between the NFA and GFA was observed for the S3 particles. Consequently, the aspect ratios appeared in the order NFA < GFA_Gr < GFA_Br < GFA_Tr, as shown in Fig. 8b. The highest aspect ratio of GFA_Tr was expected to be due to the weak glass network (low Fe_2O_3); however, further studies are required to clarify this.

The crushing rate of the NFA was higher than that of the GFA (Fig. 8b). The angular shape of the GFA can improve crushing resistance owing to the interlocking effect (Naderi et al., 2021; Shen et al., 2018; Wu et al., 2019). The crushing rate of GFA was in the order GFA_Gr < GFA_Br < GFA_Tr. The higher crushing rate of GFA_Tr was due to the weak glass network and the numerous micro-damages present in the particles.

The solubility of GFA according to the number of days immersed in a 1N NaOH solution is shown in Fig. 9. It is reported that increasing the content of Cr_2O_3 increases the bonding force and melting resistance of glass (Al-Buriahi et al., 2020; Cui et al., 2021; Eronyan et al., 2023). Therefore, the weight loss of GFA at 14 days of GFA was in the order of GFA_Gr < GFA_Br < GFA_Tr. GFA_Tr exhibited a rapid dissolution rate owing to the rapid diffusion of alkaline ions (Na^{2+} and OH^-) through numerous microdamages. Interestingly, although the weight loss was lower, GFA_Gr and GFA_Br also showed dissolution rates similar to those of GFA_Tr. This indicates that GFA_Gr and GFA_Br may also contain microcracks in their particles. This issue will be discussed in the next section.

As a result of the FA properties, the GFA showed a higher aspect ratio than the NFA. Among the GFAs, GFA_Tr showed the highest crushing rate and weight loss because of its weak glass network and microdamage. In contrast, GFA_Gr exhibited the lowest crushing rate and weight loss owing to its high content of Cr_2O_3, which improved the glass network and melting resistance. However, it is possible that microcracks in the GFA_Gr and Br particles were not observed by SEM.

4 Effect of GFA Color

4.1 Compressive and Flexural Strength

Fig. 10 shows the compressive and flexural strengths of the mortars according to the FA type. Compared with the Ref specimen, the GFA specimens had significantly reduced mortar strength regardless of color, owing to their smooth surface and high aspect ratio. The compressive and flexural strengths of the mortar according to the

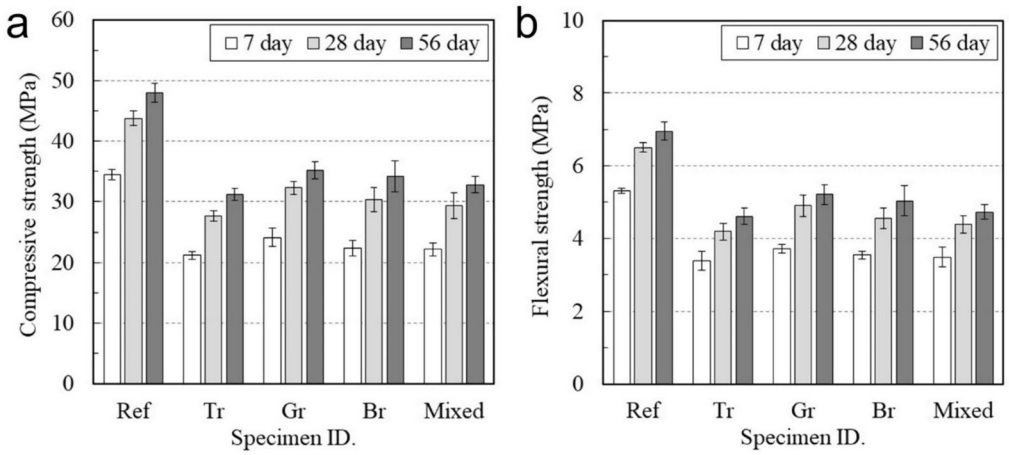

Fig. 10 Strength of mortar for color effect test (**a** Compressive, **b** Flexural)

type of GFA were in the order Tr < Mixed < Br < Gr, which was similar to that reported by Tan & Du, (2013). Among the GFAs, GFA_Gr showed the lowest aspect ratio and crushing rate and, therefore, the slightest decrease in mortar strength when replacing NFA. In contrast, GFA_Tr reduced the strength of the mortar the most owing to its high aspect ratio and crushing rate, as well as microcracks in the particles. Blending the three colors had no significant effect on the strength reduction of the mortar.

Fig. 11 shows the relative compressive and flexural strengths of the mortar compared with those of the Ref specimen. The strength development of mortars using GFA according to the curing days was higher than that of mortars using NFA. This is because the fine glass particles cause a pozzolanic reaction, as reported in other studies (Tan & Du, 2013). However, in this study, the difference in the pozzolanic reaction depending on the color of the GFA appears unclear. The relative flexural strength of the mortar prepared using GFA was slightly higher than that of the relative compressive strength. At 56 d, the relative compressive strengths of Tr, Gr, Br, and the mixture were 0.65, 0.73, 0.71, and 0.67, respectively, while the relative flexural strengths were 0.66, 0.75, 0.73, and 0.68, respectively. These results are expected because the high aspect ratio of GFA affects the cracking of the mortar owing to the flexural load (Zegardło et al., 2018).

The color effect of GFA on the mechanical properties can be summarized as follows: (1) GFA_Tr reduced the compressive and flexural strength of the mortar the most, owing to the high aspect ratio and microcracks in the particles; (2) the relatively low aspect ratio and crushing rate of GFA_Gr resulted in less reduction in the strength of the mortar; and (3) the difference in the pozzolanic reaction of GFA depending on color was unclear. These results are similar to those of some studies (Bhandari & Tajne, 2013; Tan & Du, 2013), but different from the results of other studies (Değirmenci et al., 2011; Dhir et al., 2009), in which GFA_Tr showed

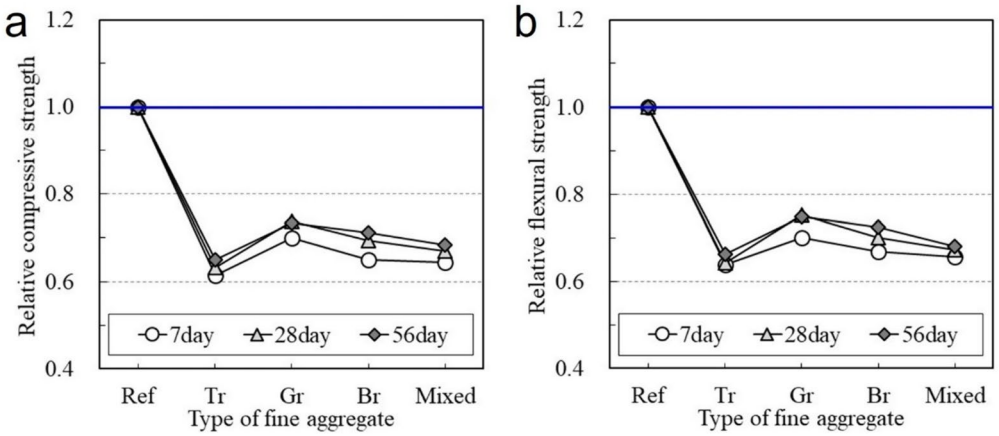

Fig. 11 Relative strength of mortar for color effect test compared to the reference mortar (**a** Compressive, **b** Flexural)

the lowest strength reduction. It is expected that the cause of these contradictory findings is the waste glass used in manufacturing GFA. In a study by Değirmenci et al., (2011), white soda-lime glass showed higher Fe_2O_3 than green. In addition, in a study by Dhir et al., (2009), in the soda-lime glass used, Fe_2O_3 was present in white, whereas it was absent in green and amber. Therefore, the chemical composition of waste glass manufactured with GFA can significantly affect the strength of the mortar, even if it is the same soda-lime glass.

4.1.1 AMBT

Fig. 12 shows the ASR expansion of mortar according to the FA type. The expansion of the Tr specimen exceeded 0.8% on day 14 and 1.5% on day 28. In particular, the ASR expansion of Tr increased rapidly from the beginning of the test; this phenomenon is similar to the solubility results (Fig. 9). These results were mainly due to microcracks in the GFA_Tr particles; the low MgO content (0.73%) may also have contributed (Bignozzi et al., 2015). The ASR expansion of the Gr and Br specimens was lower than 0.1% at 14 d but increased rapidly after 14 d. Consequently, the ASR expansions of the Gr and Br specimens exceeded 0.15 and 0.2%, respectively, at 28 days. This phenomenon appears to differ from other studies (Değirmenci et al., 2011; Du & Tan, 2013; Zhu et al., 2009) that reported low ASR expansion, even on days 14–28. The ASR expansion of the mixed specimens exceeded 0.3% at 14 d and 0.7% at 28 d. Despite the presence of GFA_Gr and Br with relatively low reactivity, the mixed specimen exhibited high ASR expansion because of the highly reactive GFA_Tr.

To determine the cause of the increased expansion of the Gr and Br specimens, the microstructure of the specimen after 14 d of AMBT was analyzed, as shown in Fig. 13. Some random microcracks observed in the matrix are likely the result of drying shrinkage that occurred during the SEM-BSE specimen preparation. In the Tr specimen, numerous cracks appeared owing to the swelling pressure of the ASR gel formed inside the glass particles (Fig. 13a). The cracks formed inside the glass particles propagated the damage through the sharp edges of the particles, promoting the formation of an ASR gel on the other glass particles (Wang et al., 2023). This chain reaction appears to have resulted in the high ASR expansion of the Tr specimen.

Compared with the Tr specimen, the Gr specimen had relatively few cracks caused by the ASR gel formed inside the glass particles (Fig. 13b). Interestingly, the ASR gel was not formed despite the presence of microcracks inside the glass particles. As shown in the solubility results (Fig. 10), GFA_Gr has a low reactivity owing to Cr_2O_3 compared to the other colors. Therefore, only a few ASR gels are expected to form through microcracks, owing to the melting resistance of GFA_Gr, until 14 days prior. The Br specimen was observed to have more cracks caused by the ASR gel formed inside the glass particles than the Gr specimen (Fig. 14c). GFA_Br showed a relatively rapid dissolution of amorphous silica by alkali ions penetrating the microcracks because the Cr_2O_3 content was lower than that of GFA_Gr (Table 1).

As a result, all GFAs had microcracks inside the particles, which caused ASR gel formation and swelling pressure. The ASR expansion of the mortar was in the order of Gr < Br < Mixed < Tr, owing to the differences in reactivity depending on the color of the GFA. Du & Tan, (2014a, 2014b) reported that GFA_Br exhibited a lower ASR expansion than GFA_Gr because of the absence of microcracks in its particles, in contrast to the results of this study. This research gap appears to be due to

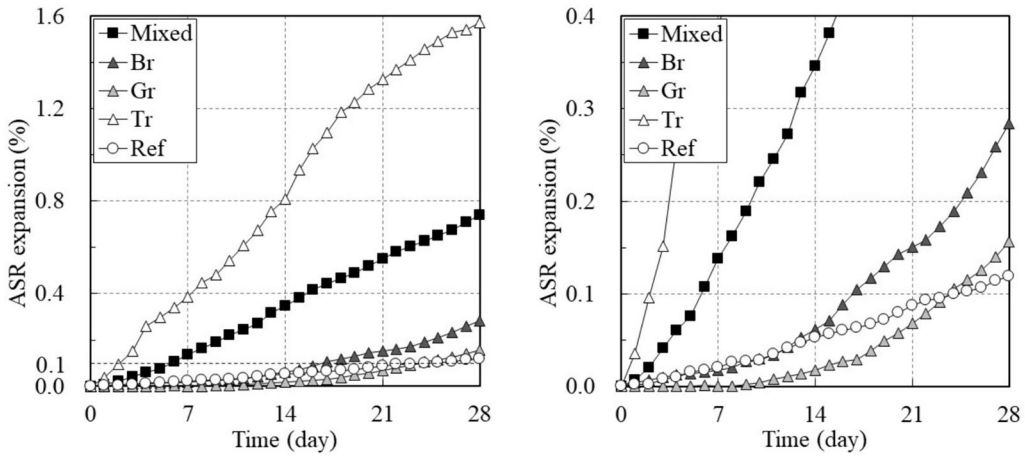

Fig. 12 ASR expansions of mortar for color effect test

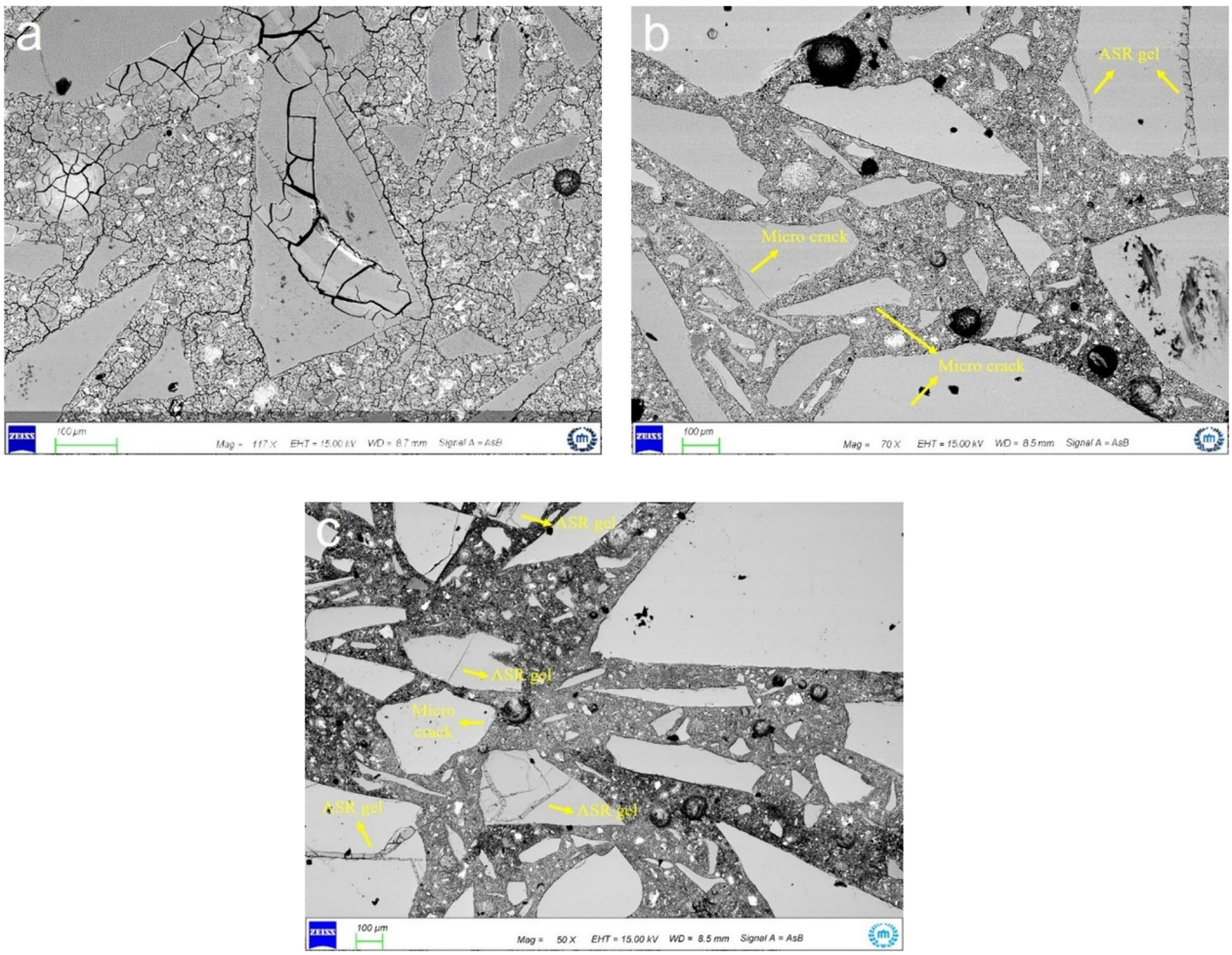

Fig. 13 SEM-BSE micrographs of mortar after 14 days of AMBT (**a** Tr, **b** Gr, **c** Br)

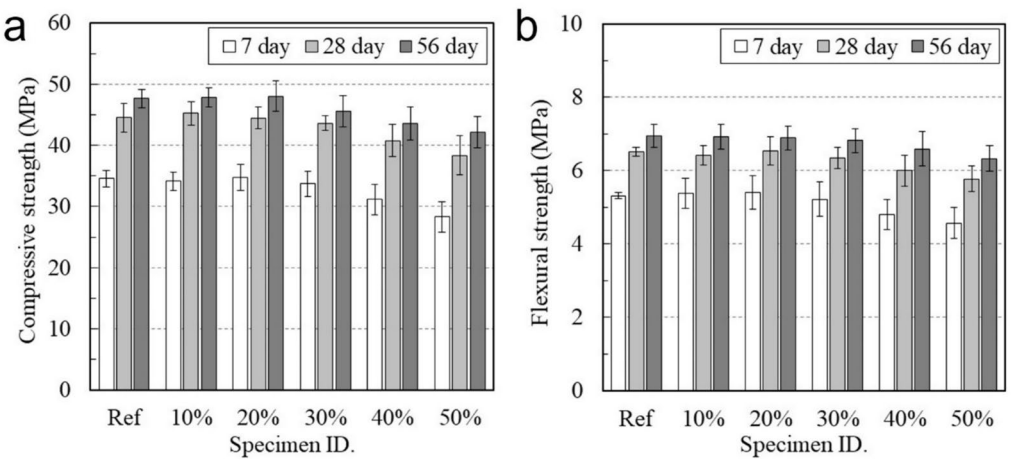

Fig. 14 Strength of mortar for content effect test (**a** Compressive, **b** Flexural)

differences in the manufacturing methods of GFA. They manufactured GFA using a jaw crusher; however, the information on whether mass production is possible is limited. Meanwhile, it was observed that ASR gel was formed through microcracks in GFA with a particle size of approximately 500 μm or more, which causes swelling pressure in this study.

4.2 Effect of GFA Content

4.2.1 Compressive and Flexural Strength

Fig. 14 shows the compressive and flexural strengths of the mortar with respect to GFA content. It was found that the effect of a GFA content lower than 30% on the compressive and flexural strengths of the mortar was unclear. On the other hand, it was found to reduce the compressive and flexural strength of the mortar when the GFA content was 30% or more. At 56 d, the compressive strengths of the 30%, 40%, and 50% specimens were 96%, 91%, and 88% of the Ref specimen, respectively. The ratios for flexural strength were 98%, 95%, and 91%. As the GFA content increased, the ITZ (which had a negative effect on strength) increased, and the distance between the GFA particles decreased, increasing the possibility of crack formation (Wang et al., 2022a, 2022b). In addition, microcracks inside the GFA particles may promote mortar cracking.

When the GFA content was 30% or less, the change in the relative strength with curing time was insignificant, as shown in Fig. 15. It appears that the pozzolanic reaction of the fine particles in the GFA (10–30% content) was not sufficient to affect the strength. However, as the GFA content increased from 30 to 50%, the relative strength according to the curing days increased compared to that of the Ref specimen. This indicates that the pozzolanic reaction of the GFA (> 30%) increased the strength of the mortar. The specimen containing 100% GFA exhibited the lowest relative strength. Notably, the strength development of the mortar using GFA (100% content) according to the number of curing days was lower than that of GFA (50% content). The excessive use of GFA can negatively affect pozzolanic reactions (Harrison et al., 2020). The agglomeration of fine particles may also have contributed to these results (Aliabdo et al., 2016).

4.2.2 AMBT

Fig. 16 shows the ASR expansion of mortar according to the GFA content. As the GFA content increased, the ASR expansion of the mortar increased. When the GFA content was 20% or less, the ASR expansion was less than 0.1% on day 14 and less than 2.0% on day 28. When the GFA content was 20% or less, the ASR expansion was less than 0.1% on day 14 and 2.0% on day 28. However, the expansion of mortars using more than 30% GFA exceeded 0.1% at 14 d and 2.0% at 28 d. These results differ from those reported in previous studies (Ismail & Al-Hashmi, 2009; Saccani & Bignozzi, 2010; Topcu & Canbaz, 2004). In this study, the GFA was found to have numerous microcracks in the particles, which is a major factor influencing ASR expansion (Du & Tan, 2014a, 2014b; Rajabipour et al., 2010). In addition, GFA_Tr contributed to these results, showing extreme ASR expansion owing to its high reactivity (Fig. 12a).

Fig. 17 shows the relative expansion of the mortar compared to that of the Ref specimen. It was found that increasing the GFA content resulted in greater ASR expansion of the mortar over the test period. The relative expansion of specimens with 10% and 50% GFA content were 1.27 and 1.39 at 4 days and 1.39 and 2.95 at 28 days, respectively. The sharp edge of the GFA is expected to

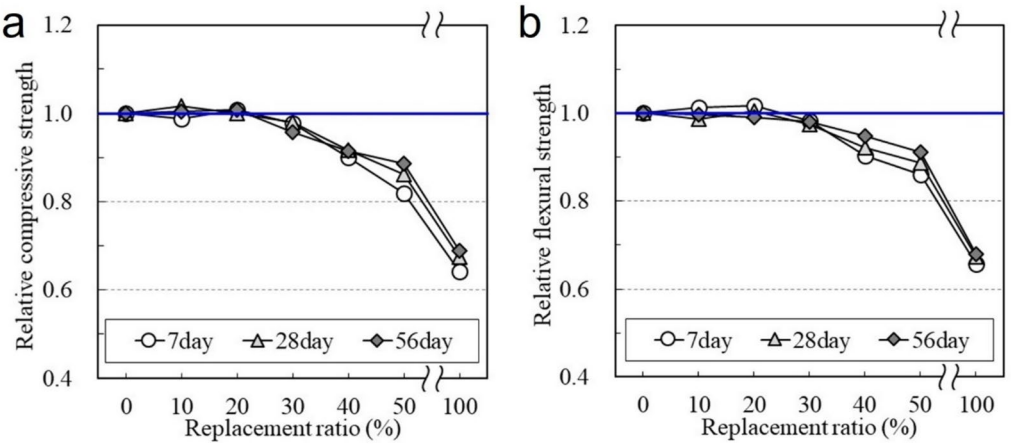

Fig. 15 Relative strength of mortar for content effect test compared to the reference mortar (**a** Compressive, **b** Flexural)

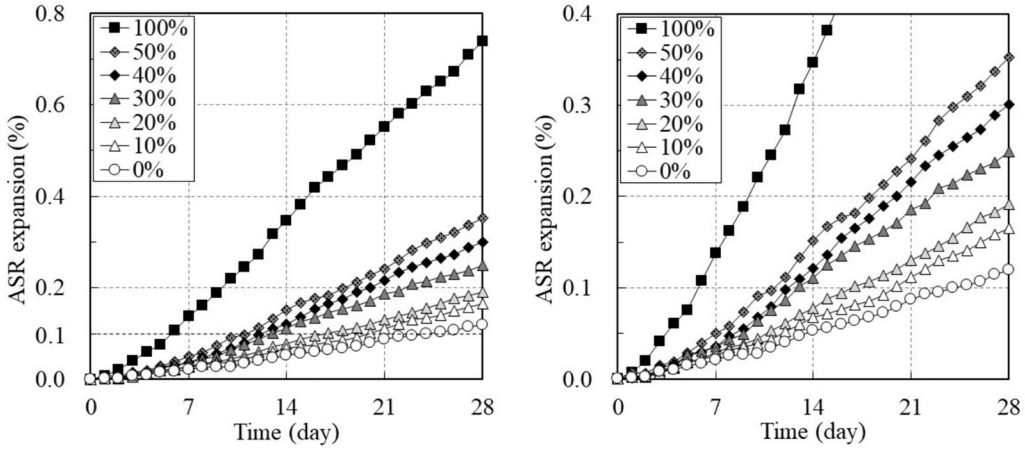

Fig. 16 ASR expansions of mortar for content effect test

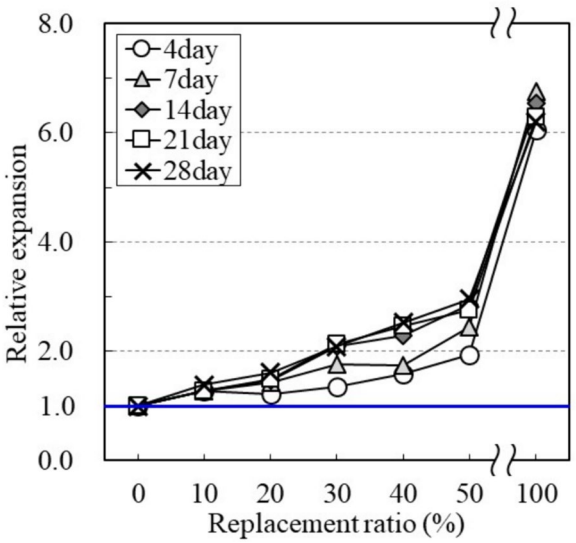

Fig. 17 Relative expansion of mortar for content effect test compared to the reference mortar

concentrate the cracking caused by the swelling pressure of the ASR gel, as shown in Fig. 13a. These cracks caused other cracks in the GFA particles and promoted ASR gel formation (Wang et al., 2023). Therefore, the increase in the angular GFA negatively affected the ASR expansion of the mortar.

It is well known that the use of GFA causes an ITZ, which has a negative effect on the strength. However, an appropriate GFA content has been reported to improve the strength of cement composites (Corinaldesi et al., 2005; Kou & Poon, 2009; Limbachiya, 2009; Penacho et al., 2014; Serpa et al., 2013). The appropriate GFA content is reported to be 10–70%, which is a wide range. Therefore, this study investigated the content of mass-produced GFA that can be used as sustainable FA. Consequently, the high aspect ratio, angular shape, and smooth surface of GFA reduced the compressive and flexural strengths of the mortar. A high GFA content (100%) had a negative effect on the pozzolanic reaction and decreased the strength of the mortar. However, the use of GFA at an appropriate content (≤20%) did not significantly reduce the strength of the mortar. The angular shapes and microcracks inside the GFA particles contributed to an increase in the ASR expansion of the mortar. Increasing the GFA content caused the mortar to exhibit a relatively greater ASR expansion according to the AMBT period. These results differ from those of previous studies (Dhir et al., 2009; Du & Tan, 2014a, 2014b; Ismail & Al-Hashmi, 2009; Zhu et al., 2009). This study used two crushing processes (hammer and roll crushing) to mass-produce GFA. This process results in the formation of microcracks in the GFA particles, which negatively affects the strength and ASR expansion of the mortar.

4.3 Effect of GFA Particle Size

4.3.1 Compressive and Flexural Strength

Fig. 18 shows the compressive and flexural strengths of the mortar with GFA particles. For the compressive strength at 56 d, specimens S1, S2, and S5 exhibited 98%, 96%, and 102% of the Ref specimens, respectively. The flexural strength ratios were 101%, 100%, and 103%, respectively. The replacement of GFA with S1, S2, and S5 particles in the NFA did not have a significant effect on the compressive and flexural strengths of the mortar. However, the S3 and S4 specimens showed a decrease in strength compared with the Ref specimens,

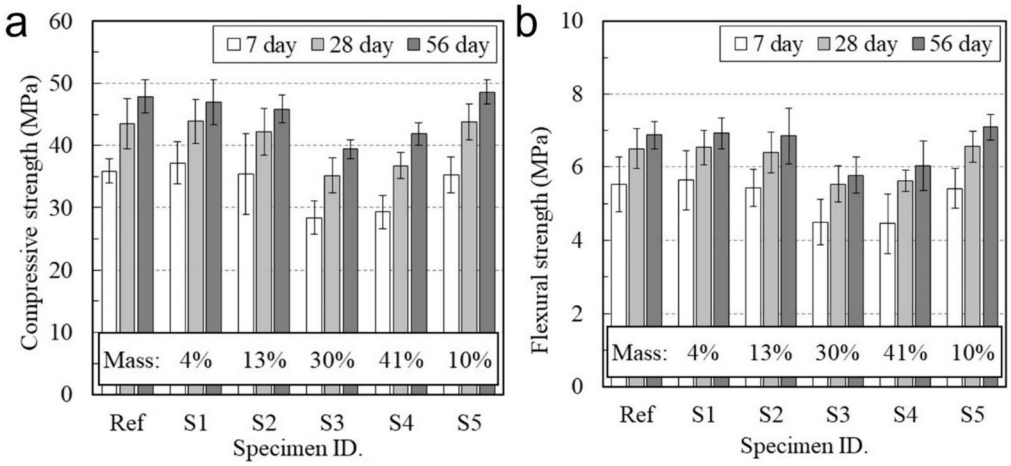

Fig. 18 Strength of mortar for particle size effect test (**a** Compressive, **b** Flexural)

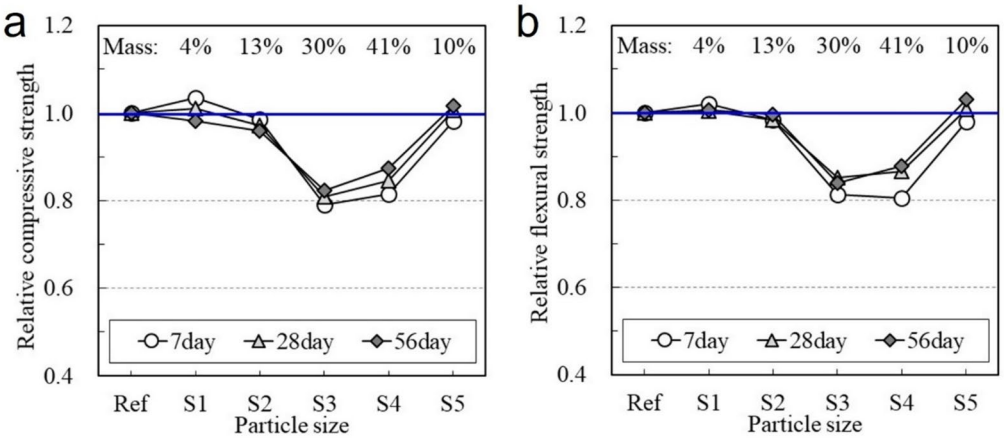

Fig. 19 Relative strength of mortar for particle size effect test compared to the reference mortar (**a** Compressive, **b** Flexural)

with compressive strengths of 82% and 87% and flexural strengths of 84% and 88%, respectively, at 56 days. Although a high GFA content reduced the strength of the mortar (Fig. 14), the S4 specimen showed a higher strength than the S3 specimen.

The relative strength of the mortar with GFA particles is shown in Fig. 19. The particle size of GFA was found to have different effects on the relative strength of the mortar according to the number of curing days. The relative strengths of specimens S1 and S2 tended to decrease as the curing time increased. This indicates that the effect of ITZ changes due to the replacement of particles (1.18–4.75 mm) in GFA is more negative at 56 days than at 7 days. In addition, the relative strength decreased significantly with curing time when the particle size fraction was larger (Wang et al., 2022a, 2022b). The S3 specimen showed a lower relative strength than the S4 specimen despite its lower GFA content. The effects that contributed to this result may be as follows: (1) a higher aspect ratio of the particles is more negative for the strength (Koh, 2014); a higher size fraction of particles is more negative for the strength (Ling & Poon, 2011); and (3) the fine particles of S4 contributed to the strength development through the pozzolanic reaction (Lee et al., 2013). Meanwhile, the relative compressive strengths of the S5 specimen after 7 and 56 days were 0.98 and 1.02, respectively. The strength development owing to the pozzolanic reaction of GFA in the S5 particles appears to be unclear at a content of 10%.

4.3.2 AMBT

Fig. 20 shows the ASR expansion of the mortar according to the GFA particle size. Except for the S5 specimen, the ASR expansions of the specimens using GFA exceeded 0.1% at 14 d and 2.0% at 28 d. Even though the GFA content was 10%, the S1 specimen showed a high

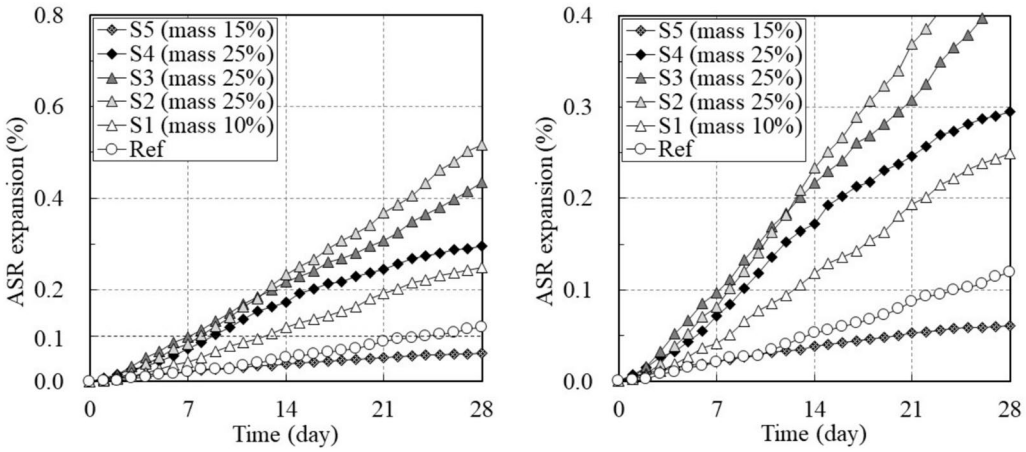

Fig. 20 ASR expansions of mortar for particle size effect test

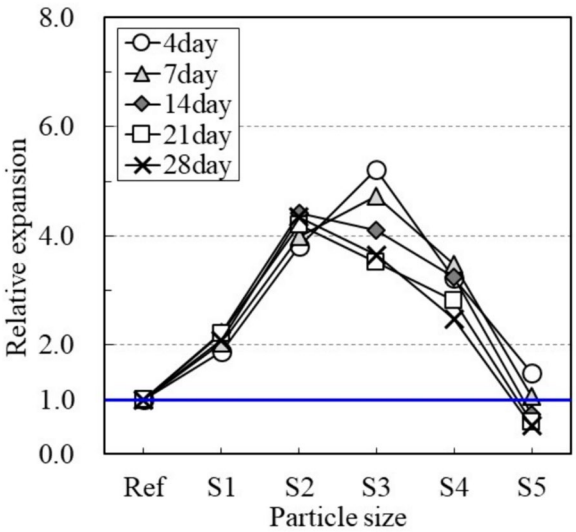

Fig. 21 Relative expansion of mortar for particle size effect test compared to the reference mortar

ASR expansion because of the large size fraction of particles in the GFA. Specimens with the same GFA content (25%) showed higher ASR expansion as the particle size fraction increased (Rajabipour et al., 2010). Interestingly, the S4 specimen showed a high ASR expansion (0.17% at 14 days and 0.3% at 28 days). In several studies (Jin et al., 2000; Rajabipour et al., 2010; Wang et al., 2023; Xie et al., 2003), the GFA of S4 particles was reported to be the "threshold size" at which ASR is suppressed owing to pozzolanic reactions. However, in this study, ASR gel due to microcracks was observed in GFA of 500 μm particles (Fig. 13c).

To clarify the effect of the GFA particle size, the relative expansion of the mortar compared to was analyzed, as shown in Fig. 21. Specimens S1 and S2 exhibited a higher relative expansion with an increasing number of test days. In this study, this result is typical because the ASR gel in the GFA promotes another ASR gel through the cracks. However, specimens S3, S4, and S5 exhibited lower relative expansion with increasing testing days. Zheng, (2016) reported that the pozzolanic reaction in glass increases the aluminum concentration in the pore solution, delaying the ASR. Therefore, these results appear to be due to the delayed ASR caused by the pozzolanic reaction of the fine GFA particles. However, in specimens S3 and S4, the pozzolanic reaction of GFA did not completely control the ASR. For GFA particles (with microcracks) larger than 500 μm, ASR expansion occurs continuously because alkaline ions that penetrate microcracks remain there and form a continuous ASR gel (Du & Tan, 2014a, 2014b).

GFA is known to have a more negative effect on strength and ASR expansion at larger size fractions. However, no cases have been confirmed in which mass-produced GFA has been used as a sustainable fine aggregate to replace NFA particles according to fineness. Therefore, in this study, the mortar strength and ASR expansion were investigated according to the particle size of mass-produced GFA. As a result, the large size fraction of GFA did not appear to have a significant effect on the strength of the mortar at a low content (4% for S1 and 13% for S2). However, the high GFA contents of the S3 and S4 particles significantly reduced the strength of the mortar. In particular, GFA (S3 particles) had the most negative effect on the strength of the mortar owing to its high aspect ratio and large size fraction. Meanwhile, a large fraction of GFA had a negative effect on the ASR expansion of the mortar. The GFA in the S1 particles caused a high ASR expansion in the mortar despite its low content (10%). The effect

of small-sized fractions (S3 and S4) of GFA on the ASR expansion of the mortars revealed interesting results. The pozzolanic reaction of fine particles of GFA appeared to delay the ASR. However, ASR is not completely controlled because ASR gel is continuously formed inside GFA particles of 500 μm or larger. Therefore, the GFA of the S4 particles, which has been reported as the threshold size in other studies (Jin et al., 2000; Rajabipour et al., 2010; Wang et al., 2023; Xie et al., 2003), had a negative effect on the ASR expansion of the mortar. This study suggested that the threshold size with insignificant effect on ASR expansion was 300–400 μm.

This study investigated the effects of color, content, and particle size to determine sustainable fine aggregate conditions for mass-produced GFA, as listed in Table 5. The sustainable fine aggregate conditions for mass-produced GFA were as follows: (1) content of color-mixed GFA within 20% and (2) content of color-mixed GFA fine particles (S5) within 15%. If the GFA_Tr content was reduced, more GFA could be used. However, the amount of GFA that can be recycled as fine aggregates is limited. Moreover, the process for the mass production of GFA generated microcracks inside the particles, which had a negative effect on the ASR expansion (Fig. 13). If ASR expansion is maintained, GFA is likely to have a deleterious effect on the durability of concrete. Effective solutions, such as using SCMs to control the ASR expansion, are required.

In this study, the effect of GFA applied under field conditions of mass production on the strength and ASR expansion behavior of mortar was analyzed. GFA under field conditions showed different results from GFA under laboratory conditions reported in other studies. Therefore, when using mass-produced GFA in concrete, it is recommended to use it as a replacement for less than 20% of NFA. However, it is expected to be difficult to use as a fine aggregate for structural concrete, due to the smooth surface and microcracks of GFA. Further research is needed to investigate the GFA effect on the properties of concrete, as the replacement within 20% is an analysis result based on mortar.

5 Conclusions

This study investigated the effects of mass-produced waste glass fine aggregate (GFA) usage on the compressive strength, flexural strength, and ASR expansion behavior of mortar. The effects of color (transparent, green, and brown), content (10, 20, 30, 40, 50, and 100%), and particle size (S1, S2, S3, S4, and S5) were investigated

Table 5 Effect of GFA on the mechanical properties and ASR expansions of mortars

Usage conditions of GFA			Compressive strength		Flexural strength		ASR expansions		
Color	**Particle size (μm)**	**Content (%)**	**28 days (%)**	**56 days (%)**	**28 days (%)**	**56 days (%)**	**14 days (%)**	**28 days (%)**	**< 0.1% at 14 days**
Trans-parent	4750–0	100	63	65	64	66	1523	1317	·
Green		100	74	73	75	75	34	131	○
Brown		100	69	71	70	72	116	238	○
Mixed		10	102	100	99	100	127	139	○
		20	100	101	101	99	146	161	○
		30	98	96	97	98	209	209	·
		40	92	91	92	95	229	252	·
		50	86	89	89	91	286	295	·
		100	67	69	67	68	654	620	·
	4750–2360	4	101	98	100	101			
		10					224	209	·
	2360–1180	13	97	96	98	100			
		25					441	434	·
	1180–600	30	81	82	85	84			
		25					410	365	·
	600–300	41	85	87	87	88			
		25					325	248	·
	300–150	10	101	102	101	103			
		15					72	51	○

"○" denotes sample did not exceed 0.1% at 14 days; "·" denotes sample exceeded 0.1% at 14 days

as usage conditions. Based on this study, the following conclusions were drawn:

1) The mass-production process caused microcracks in the GFA particles, the leading causes of mortar strength reduction and ASR expansion. Critical microcracks are observed in the transparent GFA.
2) The chemical composition of the GFA significantly affected the strength and ASR expansion of the mortar. Transparent GFA had the most negative effect on the strength and ASR expansion of the mortar owing to its relatively weak glass network and critical microcracks. Green GFA showed a relatively low strength reduction and ASR expansion owing to its relatively low aspect ratio and high melting resistance. However, after 14 d of AMBT, a rapid increase in the ASR expansion of the mortar was observed owing to microcracks in the green GFA particles.
3) The high GFA content promoted crack coalescence because of the close distance between the particles, resulting in a higher strength reduction and ASR expansion of the mortar. Moreover, a 100% GFA content had a negative effect on the pozzolanic reaction of fine glass particles. However, the appropriate GFA content did not have a significant effect on the strength or ASR expansion of the mortar, which was found to be 20% or less.
4) A large fraction of GFA particles had a deleterious effect on the strength development and ASR expansion of the mortar. In addition, the S4 particles of the GFA showed high strength reduction and ASR expansion, which were not expected to have a significant effect on the mortar owing to the pozzolanic reaction. It is assumed that these results are due to microcracks occurring in GFA particles larger than 500 μm. Therefore, the "threshold size" for mass-produced GFA is suggested to be 300–400 μm.

This study limited the usage conditions for mass-produced GFA because of its adverse effects on mortar. Future research must investigate methods, such as SCMs or surface treatments, to use large amounts of mass-produced GFA as sustainable fine aggregates. Furthermore, an economical and efficient method for mass-producing GFA without microcracks is required. These case studies are expected to accelerate the recycling of GFA as a construction material.

Acknowledgements
Not applicable.

Author contributions
Minjae Son contributed to conceptualization, methodology, experiment execution, data analysis, writing—original draft; Gyuyong Kim contributed to funding acquisition, supervision, project administration, resources, validation; Sangkyu Lee contributed to validation, writing review and editing; Hongseop Kim contributed to validation, writing review and editing; Hamin Eu contributed to experiment execution, data interpretation; Yaechan Lee contributed to experiment execution, data interpretation; Sasui Sasui contributed to validation, writing review and editing; Jeongsoo Nam contributed to resources, supervision. All the authors read and approved the final manuscript.

Funding
This work was supported by the National Research Foundation of Korea (NRF) grant funded by the Korea government (MSIT) (No. RS-2023-00220921).

Availability of data and materials
The datasets used and/or analysed during the current study are available from the corresponding author on reasonable request.

Declarations

Competing interests
The authors declare that they have no competing interests.

Received: 28 February 2024 Accepted: 8 May 2024
Published online: 22 August 2024

References

Al-Buriahi, M. S., Alajerami, Y. S. M., Abouhaswa, A. S., Alalawi, A., Nutaro, T., & Tonguc, B. (2020). Effect of chromium oxide on the physical, optical, and radiation shielding properties of lead sodium borate glasses. *Journal of Non-Crystalline Solids, 544*, 120171. https://doi.org/10.1016/j.jnoncrysol.2020.120171

Aliabdo, A. A., Abd Elmoaty, M., & Aboshama, A. Y. (2016). Utilization of waste glass powder in the production of cement and concrete. *Construction and Building Materials, 124*, 866–877. https://doi.org/10.1016/j.conbuildmat.2016.08.016

ASTM C 1260-14. (2014). *Standard test method for potential reactivity of aggregates (Mortar-Bar Method)*. West Conshohocken: ASTM International.

Bhandari, P., & Tajne, K. M. (2013). Use of waste glass in cement mortar. *International Journal of Civil & Structural Engineering, 3*(4), 704–711. https://doi.org/10.6088/ijcser.201203013064

Bignozzi, M. C., Saccani, A., Barbieri, L., & Lancellotti, I. (2015). Glass waste as supplementary cementing materials: The effects of glass chemical composition. *Cement and Concrete Composites, 55*, 45–52. https://doi.org/10.1016/j.cemconcomp.2014.07.020

Bilodeau, A., & Malhotra, V. M. (2000). High-volume fly ash system: concrete solution for sustainable development. *Materials Journal, 97*(1), 41–48. https://doi.org/10.14359/804

Bisht, K., & Ramana, P. V. (2018). Sustainable production of concrete containing discarded beverage glass as fine aggregate. *Construction and Building Materials, 177*, 116–124. https://doi.org/10.1016/j.conbuildmat.2018.05.119

Charles, R. J. (1958). Static fatigue of glass. II. *Journal of Applied Physics, 29*(11), 1554–1560. https://doi.org/10.1063/1.1722992

Corinaldesi, V., Gnappi, G., Moriconi, G., & Montenero, A. J. W. M. (2005). Reuse of ground waste glass as aggregate for mortars. *Waste Management, 25*(2), 197–201. https://doi.org/10.1016/j.wasman.2004.12.009

Cui, K., Zhang, Y., Fu, T., Hussain, S., Saad Algarni, T., Wang, J., & Ali, S. (2021). Effects of Cr_2O_3 content on microstructure and mechanical properties of Al_2O_3 matrix composites. *Coatings, 11*(2), 234. https://doi.org/10.3390/coatings11020234

Dadouch, M., Belal, T., & Ghembaza, M. S. (2024). Valorization of glass waste as partial substitution of sand in concrete–Investigation of the physical and mechanical properties for a sustainable construction. *Construction and Building Materials, 411*, 134436. https://doi.org/10.1016/j.conbuildmat.2023.134436

Değirmenci, N., Yılmaz, A., & Çakır, Ö. A. (2011). Utilization of waste glass as sand replacement in cement mortar. Retrieved from https://hdl.handle.net/20.500.12462/7135

Dhir, R. K., Dyer, T. D., & Tang, M. C. (2009). Alkali-silica reaction in concrete containing glass. *Materials and Structures, 42*, 1451–1462. https://doi.org/10.1617/s11527-008-9465-8

Du, H., & Tan, K. H. (2013). Use of waste glass as sand in mortar: Part II–Alkali–silica reaction and mitigation methods. *Cement and Concrete Composites, 35*(1), 118–126. https://doi.org/10.1016/j.cemconcomp.2012.08.029

Du, H., & Tan, K. H. (2014a). Effect of particle size on alkali–silica reaction in recycled glass mortars. *Construction and Building Materials, 66*, 275–285. https://doi.org/10.1016/j.conbuildmat.2014.05.092

Du, H., & Tan, K. H. (2014). Concrete with recycled glass as fine aggregates. *ACI Mater Journal, 111*(1), 47–58. https://doi.org/10.14359/51686446

Eronyan, M. A., Parfenov, P. S., Kulesh, A. Y., Meshkovskiy, I. K., & Untilov, A. A. (2023). Cr_2O_3 doping effect on silica glass cooling rate. *Silicon, 15*(8), 3479–3483. https://doi.org/10.1007/s12633-022-02268-4

Eu, H., Kim, G., Yoon, G., Lee, Y., Sasui, S., Son, M., & Nam, J. (2024). Field experiment on performance of water source heat pump using underground rainwater tank as heat source. *Journal of Building Engineering*. https://doi.org/10.1016/j.jobe.2024.108551

Guinea, G. V., El-Sayed, K., Rocco, C. G., Elices, M., & Planas, J. (2002). The effect of the bond between the matrix and the aggregates on the cracking mechanism and fracture parameters of concrete. *Cement and Concrete Research, 32*(12), 1961–1970. https://doi.org/10.1016/S0008-8846(02)00902-X

Guo, P., Meng, W., Nassif, H., Gou, H., & Bao, Y. (2020). New perspectives on recycling waste glass in manufacturing concrete for sustainable civil infrastructure. *Construction and Building Materials, 257*, 119579. https://doi.org/10.1016/j.conbuildmat.2020.119579

Hamada, H., Alattar, A., Tayeh, B., Yahaya, F., & Thomas, B. (2022). Effect of recycled waste glass on the properties of high-performance concrete: A critical review. *Case Studies in Construction Materials, 17*, e01149. https://doi.org/10.1016/j.cscm.2022.e01149

Harrison, E., Berenjian, A., & Seifan, M. (2020). Recycling of waste glass as aggregate in cement-based materials. *Environmental Science and Ecotechnology, 4*, 100064. https://doi.org/10.1016/j.ese.2020.100064

Idir, R., Cyr, M., & Tagnit-Hamou, A. (2010). Use of fine glass as ASR inhibitor in glass aggregate mortars. *Construction and Building Materials, 24*(7), 1309–1312. https://doi.org/10.1016/j.conbuildmat.2009.12.030

Ismail, Z. Z., & Al-Hashmi, E. A. (2009). Recycling of waste glass as a partial replacement for fine aggregate in concrete. *Waste Management, 29*(2), 655–659. https://doi.org/10.1016/j.wasman.2008.08.012

Jiang, S., Shen, L., & Li, W. (2021). An experimental study of aggregate shape effect on dynamic compressive behaviours of cementitious mortar. *Construction and Building Materials, 303*, 124443. https://doi.org/10.1016/j.conbuildmat.2021.124443

Jin, W., Meyer, C., & Baxter, S. (2000). "Glascrete"-concrete with glass aggregate. *ACI Materials Journal, 97*(2), 208–213. https://doi.org/10.14359/825

Kaewkhao, J., Siriprom, W., Insiripong, S., Ratana, T., Kedkaew, C., & Limsuwan, P. (2011). Structural and magnetic properties of glass doped with iron oxide. *In Journal of Physics Conference Series, 266*(1), 012012. https://doi.org/10.1088/1742-6596/266/1/012012

Khan, M. N. N., Saha, A. K., & Sarker, P. K. (2020). Reuse of waste glass as a supplementary binder and aggregate for sustainable cement-based construction materials: A review. *Journal of Building Engineering, 28*, 101052. https://doi.org/10.1016/j.jobe.2019.101052

Koh, C. J. (2014). Characterisation of shape of fine recycled crushed coloured glass and the effect on the properties of structural concrete when used as a fine aggregate replacement. Retrieved from http://hdl.handle.net/2436/561256

Korea Agency for Technology and Standards (KATS). (2007). KS F 2527 Concrete Aggregate.

Korea Agency for Technology and Standards (KATS). (2022). Standard test method for determination of Aggregate-Crushing-Value (ACV).

Kou, S. C., & Poon, C. S. (2009). Properties of self-compacting concrete prepared with recycled glass aggregate. *Cement and Concrete Composites, 31*(2), 107–113. https://doi.org/10.1016/j.cemconcomp.2008.12.002

Lee, G., Poon, C. S., Wong, Y. L., & Ling, T. C. (2013). Effects of recycled fine glass aggregates on the properties of dry–mixed concrete blocks. *Construction and Building Materials, 38*, 638–643. https://doi.org/10.1016/j.conbuildmat.2012.09.017

Lee, H., Kim, K., & Lee, H. (2023). The process development of cullet and recycled glass aggregate for improving waste glass bottles recycling rate. *Journal of Material Cycles and Waste Management, 25*(6), 3217–3227. https://doi.org/10.1007/s10163-023-01725-5

Li, X., Zang, X., Xing, X., Li, J., Ma, Y., & Li, T. (2022). Effect of Fe_2O_3 on the crystallization behavior of glass-ceramics produced from secondary nickel slag. *Metals, 12*(1), 164. https://doi.org/10.3390/met12010164

Limbachiya, M. C. (2009). Bulk engineering and durability properties of washed glass sand concrete. *Construction and Building Materials, 23*(2), 1078–1083. https://doi.org/10.1016/j.conbuildmat.2008.05.022

Ling, T. C., & Poon, C. S. (2011). Properties of architectural mortar prepared with recycled glass with different particle sizes. *Materials and Design, 32*(5), 2675–2684. https://doi.org/10.1016/j.matdes.2011.01.011

Matsumoto, N., Ogawa, M., Takayasu, K., Hirayama, M., Miura, T., Shiozawa, K., & Udagawa, S. (2015). Quantitative sonographic image analysis for hepatic nodules: a pilot study. *Journal of Medical Ultrasonics, 42*, 505–512. https://doi.org/10.1007/s10396-015-0627-3

Naderi, S., Tu, W., & Zhang, M. (2021). Meso-scale modelling of compressive fracture in concrete with irregularly shaped aggregates. *Cement and Concrete Research, 140*, 106317. https://doi.org/10.1016/j.cemconres.2020.106317

Park, S. B., & Lee, B. C. (2004). Studies on expansion properties in mortar containing waste glass and fibers. *Cement and Concrete Research, 34*(7), 1145–1152. https://doi.org/10.1016/j.cemconres.2003.12.005

Penacho, P., de Brito, J., & Veiga, M. R. (2014). Physico-mechanical and performance characterization of mortars incorporating fine glass waste aggregate. *Cement and Concrete Composites, 50*, 47–59. https://doi.org/10.1016/j.cemconcomp.2014.02.007

Rajabipour, F., Maraghechi, H., & Fischer, G. (2010). Investigating the alkali-silica reaction of recycled glass aggregates in concrete materials. *Journal of Materials in Civil Engineering, 22*(12), 1201–1208. https://doi.org/10.1061/(ASCE)MT.1943-5533.000012

Saccani, A., & Bignozzi, M. C. (2010). ASR expansion behavior of recycled glass fine aggregates in concrete. *Cement and Concrete Research, 40*(4), 531–536. https://doi.org/10.1016/j.cemconres.2009.09.003

Sasui, S., Kim, G., Nam, J., van Riessen, A., & Hadzima-Nyarko, M. (2021). Effects of waste glass as a sand replacement on the strength and durability of fly ash/GGBS based alkali activated mortar. *Ceramics International, 47*(15), 21175–21196. https://doi.org/10.1016/j.ceramint.2021.04.121

Sasui, S., Kim, G., Nam, J., van Riessen, A., Hadzima-Nyarko, M., Choe, G., & Jinwuth, W. (2022). Effects of waste glass sand on the thermal behavior and strength of fly ash and GGBS based alkali activated mortar exposed to elevated temperature. *Construction and Building Materials, 316*, 125864. https://doi.org/10.1016/j.conbuildmat.2021.125864

Serpa, D., Silva, A. S., de Brito, J., Pontes, J., & Soares, D. (2013). ASR of mortars containing glass. *Construction and Building Materials, 47*, 489–495. https://doi.org/10.1016/j.conbuildmat.2013.05.058

Shao, Y., Lefort, T., Moras, S., & Rodriguez, D. (2000). Studies on concrete containing ground waste glass. *Cement and Concrete Research, 30*(1), 91–100. https://doi.org/10.1016/S0008-8846(99)00213-6

Shayan, A., & Xu, A. (2004). Value-added utilisation of waste glass in concrete. *Cement and Concrete Research, 34*(1), 81–89. https://doi.org/10.1016/S0008-8846(03)00251-5

Shen, W., Liu, Y., Wang, Z., Cao, L., Wu, D., Wang, Y., & Ji, X. (2018). Influence of manufactured sand's characteristics on its concrete performance. *Construction and Building Materials, 172*, 574–583. https://doi.org/10.1016/j.conbuildmat.2018.03.139

Shi, C., & Zheng, K. (2007). A review on the use of waste glasses in the production of cement and concrete. *Resources, Conservation and Recycling, 52*(2), 234–247. https://doi.org/10.1016/j.resconrec.2007.01.013

Siddique, R. (2008). *Waste glass. Waste Materials and by-products in concrete* (pp. 147–175). Springer, Berlin Heidelberg: Springer. https://doi.org/10.1007/978-3-540-74294-4_5

Son, M., Kim, G., Kim, H., Lee, S., Lee, Y., Nam, J., & Kobayashi, K. (2021). Effect of fiber blending ratio on the tensile properties of steel fiber hybrid reinforced cementitious composites under different strain rates. *Materials, 14*(16), 4504. https://doi.org/10.3390/ma14164504

Soroushian, P., & Sufyan-Ud-Din, M. (2021). Long-term field performance of concrete produced with powder waste glass as partial replacement of

cement. *Case Studies in Construction Materials, 15*, e00745. https://doi.org/10.1016/j.cscm.2021.e00745
Standard ASTM C109. (2008). *standard test method for compressive strength of hydraulic cement mortars*. West Conshohocken: ASTM International.
Standard ASTM C348. (2008). *Standard test method for flexural strength of hydraulic-cement mortars*. West Conshohocken: ASTM International.
Taha, B., & Nounu, G. (2008). Properties of concrete contains mixed colour waste recycled glass as sand and cement replacement. *Construction and Building Materials, 22*(5), 713–720. https://doi.org/10.1016/j.conbuildmat.2007.01.019
Taha, B., & Nounu, G. (2009). Utilizing waste recycled glass as sand/cement replacement in concrete. *Journal of Materials in Civil Engineering, 21*(12), 709–721. https://doi.org/10.1061/(ASCE)0899-1561(2009)21:12(709)
Tamanna, N., Tuladhar, R., & Sivakugan, N. (2020). Performance of recycled waste glass sand as partial replacement of sand in concrete. *Construction and Building Materials, 239*, 117804. https://doi.org/10.1016/j.conbuildmat.2019.117804
Tan, K. H., & Du, H. (2013). Use of waste glass as sand in mortar: Part I-Fresh, mechanical and durability properties. *Cement and Concrete Composites, 35*(1), 109–117. https://doi.org/10.1016/j.cemconcomp.2012.08.028
Topçu, İB., Boğa, A. R., & Bilir, T. (2008). Alkali–silica reactions of mortars produced by using waste glass as fine aggregate and admixtures such as fly ash and Li_2CO_3. *Waste Management, 28*(5), 878–884. https://doi.org/10.1016/j.wasman.2007.04.005
Topcu, I. B., & Canbaz, M. (2004). Properties of concrete containing waste glass. *Cement and Concrete Research, 34*(2), 267–274. https://doi.org/10.1016/j.cemconres.2003.07.003
Wang, T., San Nicolas, R., Kashani, A., & Ngo, T. (2022a). Sustainable utilisation of low-grade and contaminated waste glass fines as a partial sand replacement in structural concrete. *Case Studies in Construction Materials, 16*, e00794. https://doi.org/10.1016/j.cscm.2021.e00794
Wang, T., San Nicolas, R., Nguyen, T. N., Kashani, A., & Ngo, T. (2022b). Mechanical behaviour of glass-mortar under uniaxial compression loading based on a meso-scale modelling approach. *Construction and Building Materials, 359*, 129499. https://doi.org/10.1016/j.conbuildmat.2022.129499
Wang, T., San Nicolas, R., Nguyen, T. N., Kashani, A., & Ngo, T. (2023). Experimental and numerical study of long-term alkali-silica reaction (ASR) expansion in mortar with recycled glass. *Cement and Concrete Composites, 139*, 105043. https://doi.org/10.1016/j.cemconcomp.2023.105043
Wu, H. L., Yu, J., Zhang, D., Zheng, J. X., & Li, V. C. (2019). Effect of morphological parameters of natural sand on mechanical properties of engineered cementitious composites. *Cement and Concrete Composites, 100*, 108–119. https://doi.org/10.1016/j.cemconcomp.2019.04.007
Xie, Z., Xiang, W., & Xi, Y. (2003). ASR potentials of glass aggregates in water-glass activated fly ash and portland cement mortars. *Journal of Materials in Civil Engineering, 15*(1), 67–74. https://doi.org/10.1061/(ASCE)0899-1561(2003)15:1(67)
Yamada, K., & Ishiyama, S. (2005). Maximum dosage of glass cullet as fine aggregate in mortar. In R. K. Dhir, T. D. Dyer, & M. D. Newlands (Eds.), *Achieving sustainability in construction: Proceedings of the International Conference held at the University of Dundee, Scotland, UK on 5–6 July 2005* (pp. 185–192). London: Thomas Telford Publishing. https://doi.org/10.1680/asic.34044.0022
Yuksel, C., Ahari, R. S., Ahari, B. A., & Ramyar, K. (2013). Evaluation of three test methods for determining the alkali–silica reactivity of glass aggregate. *Cement and Concrete Composites, 38*, 57–64. https://doi.org/10.1016/j.cemconcomp.2013.03.002
Zegardło, B., Szeląg, M., Ogrodnik, P., & Bombik, A. (2018). Physico-mechanical properties and microstructure of polymer concrete with recycled glass aggregate. *Materials, 11*(7), 1213. https://doi.org/10.3390/ma11071213
Zheng, K. (2016). Pozzolanic reaction of glass powder and its role in controlling alkali–silica reaction. *Cement and Concrete Composites, 67*, 30–38. https://doi.org/10.1016/j.cemconcomp.2015.12.008
Zhu, H., Chen, W., Zhou, W., & Byars, E. A. (2009). Expansion behaviour of glass aggregates in different testing for alkali-silica reactivity. *Materials and Structures, 42*, 485–494. https://doi.org/10.1617/s11527-008-9396-4

Publisher's Note

Minjae Son is ph.D in Department of Future & Smart Construction Research, Korea Institute of Civil Engineering and Building Technology, Goyang, Republic of Korea.

Gyuyong Kim is Professor in Department of Smart City Architectural Engineering, College of Engineering at Chungnam National University, Daejeon, Republic of Korea.

Sangkyu Lee is ph.D in Korea Construction Standards Center, Korea Institute of Civil Engineering and Building Technology, Goyang, Republic of Korea.

Hongseop Kim is ph.D in Department of Building Research, Korea Institute of Civil Engineering and Building Technology, Goyang, Republic of Korea.

Hamin Eu is Doctoral course student in Department of Architectural Engineering, College of Engineering at Chungnam National University, Daejeon, Republic of Korea.

Yaechan Lee is Doctoral course student in Department of Architectural Engineering, College of Engineering at Chungnam National University, Daejeon, Republic of Korea.

Sasui Sasui is research professor in Department of Architectural Engineering, College of Engineering at Chungnam National University, Daejeon, Republic of Korea.

Jeongsoo Nam is Assistant Professor in Department of Smart City Architectural Engineering, College of Engineering at Chungnam National University, Daejeon, Republic of Korea.